SCIENTIFIC REPORTS

OPEN

SUBJECT AREAS:
ELECTRONIC AND SPINTRONIC DEVICES
ELECTRONICS, PHOTONICS AND DEVICE PHYSICS

Received
25 July 2014

Accepted
1 September 2014

Published
29 September 2014

Correspondence and requests for materials should be addressed to P.Z. (pengzhou@fudan.edu.cn)

* These authors contributed equally to this work.

Direct Deposition of Uniform High-κ Dielectrics on Graphene

Peng Zhou*, Songbo Yang, Qingqing Sun, Lin Chen*, Pengfei Wang, Shijin Ding & David Wei Zhang

ASIC & System State Key Lab, School of Microelectronics, Fudan University, Shanghai 200433, China.

High quality High-κ dielectrics on graphene were achieved by atomic layer deposition directly using remote oxygen plasma surface pretreatment. The uniform coverage on graphene is illustrated by atomic force microscopy and confirmed by high resolution transmission microscopy. The possible surface lattice damage induced by plasma is limited and demonstrated by Raman spectra. The excellent Hall mobility for graphene is maintained at 2.7 × 10^3 $cm^2/V·s$, which only decreases by 25%. The excellent electrical characteristic of dielectric presents the low leakage current density and high breakdown voltage. Moreover, the technology is compatible with the traditional CMOS process which brings much possibility to future graphene devices.

The emerging extensive application of graphene attracts intensive attention as a promising material for future nano-electronics with high intrinsic carrier mobility[1–3]. The high quality graphene/oxide interface is critical to electronic devices such as radio-frequency transistor[4,5] and flexible electronics[6,7]. A lot of efforts have been made to realize atomic layer deposition (ALD) of high-κ dielectrics with high quality on the top of graphene. With the help of a functionalization layer of NO_2-trimetdhylaluminum (TMA)[8] or using different ultra-thin metal films as a nucleation layer to enable the ALD process[9,10], the Al_2O_3 has been successfully deposited on graphene indirectly. Recently, high-κ dielectrics have been achieved on graphene through spin-coating a polymer buffer layer in advance, which has less degradation for the carrier mobility[11,12]. Although these methods have provided successful dielectric deposition on graphene, the high quality graphene/oxide interface is still not obtained especially on the optimization electrical characteristics. The introduction of polymer and the indirect fabrication process will not only reduce the thermal budget of the device but also be incompatible with the traditional CMOS process, which limits the application seriously. Additionally, to achieve better graphene/oxide interfaces, understanding the physical nature of the dynamic deposition process is very important. However, clear clarification is still lacking in literature.

In this letter, we have developed a method for the formation of high quality uniform graphene/oxide interface directly by ALD deposition with remote oxygen plasma treatment. We report only 25% degradation in carrier mobility after optimized dielectric deposition with >1.2 MV/cm dielectric breakdown electrical field intensity and $<10^{-7}$ A/cm^2 leakage current density. In this investigation, we propose the physical images of the dielectric deposition process by ALD via remote oxygen plasma and the results of in-situ x-ray photoelectron spectroscopy (XPS) analysis verified the mechanism.

Results

The atomic force microscope (AFM) image of a 5 μm × 5 μm area is shown in Fig. 1(a). Before dielectric is deposited, there are some ripples on graphene surface which is inevitable because of the transferring graphene to a silicon substrate process and surface roughness is about 1.28 nm[13]. After the remote plasma pretreatment and the following deposition, good conformal coverage of Al_2O_3 with few pinholes is observed, as shown in Fig. 1(b). The ripples are less obvious and the surface roughness decreases to 0.90 nm which indicates the uniform Al_2O_3 film coating. As illustrated in HRTEM cross-sectional images of Fig. 2, the Al_2O_3 is confirmed on the top of graphene surface and an interfacial layer between graphene and dielectric is found. The Al_2O_3 thickness is about 18.4 nm which is in accordance with the growth rate of the Al_2O_3 ALD process. An interfacial layer between graphene and oxide is observed and the thickness is about 2 nm.

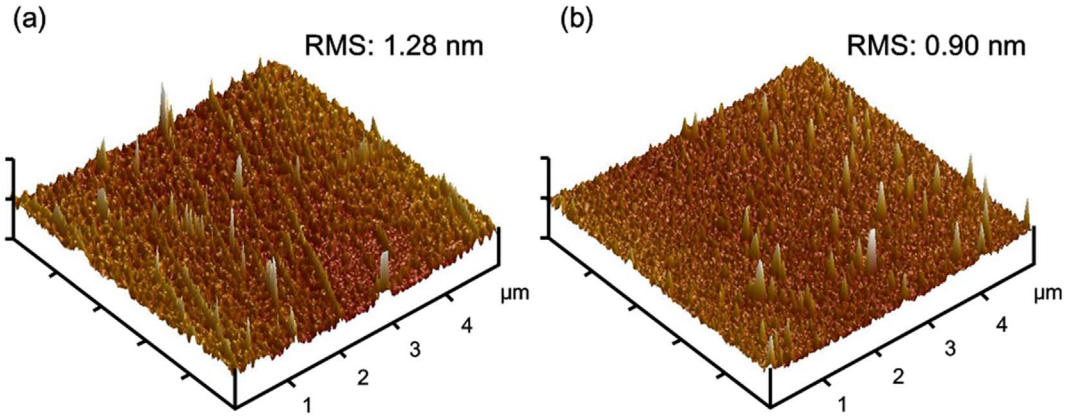

Figure 1 | **AFM images of graphene (a) before and (b) after deposited Al2O3 via O_2 plasma surface pretreated ALD process.**

Representative Raman spectra were measured (with a 514 nm laser) before and after dielectric deposition, as shown in Fig. 3. Common features of graphene, the G and 2D peaks, which lie at around 1580 cm^{-1} and 2700 cm^{-1} are observed[14,15]. Before ALD process, the D band (~1345 cm^{-1}) is not found in the spectrum which implies the transferring process doesn't bring in many disorders to graphene on silicon substrate. After the oxygen plasma surface pretreatment and ALD Al_2O_3, a low disorder-induced D band occurs which indicates defects were introduced during the process[16]. A shift of 2D peak is observed after Al_2O_3 deposition, which confirms that the doping effect occurs on graphene. The doping level of graphene can be estimated. The remote O_2 plasma pretreatment before ALD can introduce some active oxygen-containing functional groups to graphene surface forming nucleation sites to make the subsequent ALD reaction easier. However, these functional groups will also break the sp2 hybridization and bring in some disorders which may lead to the appearance of D band. As shown in blue in Fig. 3, though the O_2 plasma exposure and ALD process induce disorders in graphene, the D/G intensity ratio is less than 0.1 which still indicates limited damage and good quality of graphene surface[17,18].

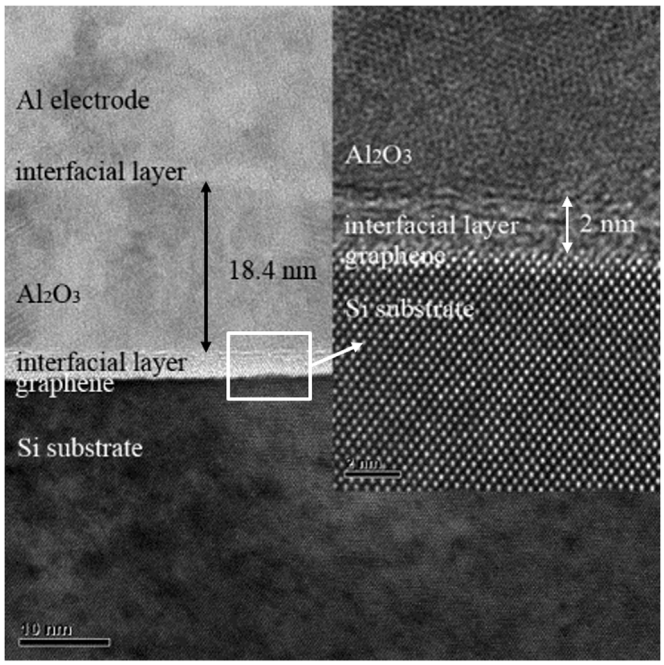

Figure 2 | **HRTEM images of the cross-sectional Al/Al2O3/graphene/Si structure.**

The Hall effect measurements were performed with the Van der Pauw method. In order to eliminate the contribution for mobility of the substrate, we use a 1 cm × 1 cm graphene sample on SiO_2 substrate and the transferring steps are the same as before. The Hall mobility for graphene transferred on SiO_2 substrate is about 3.606×10^3 $cm^2/(V \cdot s)$. After oxygen plasma pretreatment and ALD process, the measured Hall mobility reduces to 2.705×10^3 $cm^2/(V \cdot s)$. The decrease of Hall mobility is reasonable since the break of sp_2 hybridization during O_2 plasma exposure and the interfacial scattering, but compared to the Hall mobility before ALD, the 25% reduction is still acceptable.

In order to further evaluate the dielectric, top Al electrodes were manufactured by means of physical vapor deposition (PVD) for Al_2O_3/graphene/highly-doped silicon structure. I–V measurements were conducted by biasing top electrodes from 0 to 5 V at a ramp rate of 0.01 V/s. Fig. 4 shows the current density (J) varies with the electric field (E). The sample presents the leakage current is about 10^{-7} A/cm^2 before breakdown which indicates the good insulation effect of Al_2O_3 dielectric. The leakage current is probably attributed to the trap-assisted tunneling mechanism. Electrons are injected from interfacial traps to the oxygen vacancies near the interface, and the thermionic field emission of electrons between the oxygen vacancies could form a conductive path for electrons to leak[19]. At a large bias, the current increases quickly by 3 or 4 orders of magnitude and reaches the compliance limit (1 mA). The breakdown occurs at 1.2 MV/cm which is smaller than the Al_2O_3 breakdown field[20]. We attribute the phenomenon to the interfacial contact between graphene and Al_2O_3. Defects formed at interface between the graphene and dielectric could lead to early breakdown of Al_2O_3. The insert picture (b) of Fig. 4 shows the C-V measurement of the structure. The value of the dielectric constant is 8.73, which further confirms that good gate dielectrics are formed on graphene by direct atomic layer deposition.

Discussion

Fig. 5(a) shows the dynamic mechanism of Al_2O_3 dielectric forming on the top of graphene by remote oxygen plasma pretreated ALD. The oxygen plasma firstly generates remotely. After the oxygen plasma process, both the C-O bond and C = O bond are formed on the graphene surface and edge which change the graphene surface from hydrophobic to hydrophilic and make the

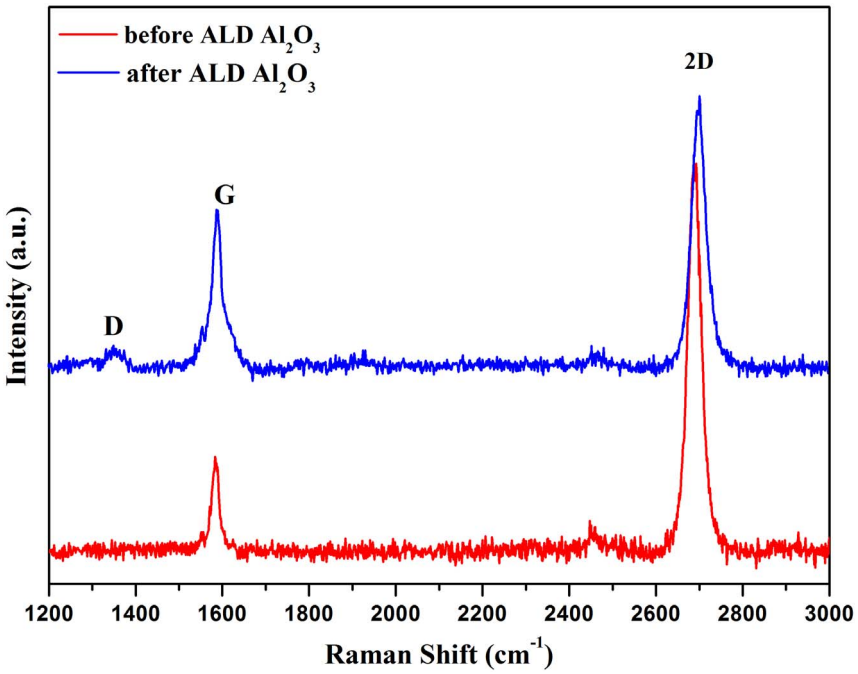

Figure 3 | **Raman spectra of graphene before (red line) and after (blue line) ALD Al_2O_3 with O_2 plasma pretreatment.**

following ALD process easier to happen. In order to prove the mechanism, we performed in-situ XPS analysis of C 1 s of graphene surface before and after oxygen plasma is introduced to surface. The Fig. 5(b) shows a single C-C peak located at 284.8 eV which indicates high quality graphene before plasma pretreatment[21]. After remote oxygen plasma is flown to surface, as shown in Fig. 5(c), the C-O peak (286.6 eV) and C(O)O peak (289.3 eV) are observed which indicates the transformation of sp_2 hybridization to sp_3 hybridization[22]. The C-O bond and C(O)O bond induced by oxygen plasma create the precondition for ALD process at the sacrifice of breaking the two-dimensional planar crystal structure and decreasing the mobility. However, by careful controlling of plasma exposure time and adjusting sp_3/sp_2 ratio, we can realize ALD high quality dielectric on the surface of graphene with introducing only limited damage.

In summary, we successfully deposited ~18.4 nm Al_2O_3 dielectric on graphene after 200 ALD cycles. The uniform coverage with the roughness of 0.9 nm and good graphene/oxide interface are confirmed by AFM and HRTEM. Since the O_2 plasma is generated remotely and the time for exposure is well-controlled during the process, the damage introduced to graphene lattice is limited which is revealed by Raman spectra. As a result, only 25% degradation of Hall mobility was detected by this method. Furthermore, we fabricated the top electrodes for Al_2O_3/graphene/highly-doped silicon structure to evaluate the electrical characteristic. A low leakage current density of 10^{-7} A/cm^2 which indicates good insulation effect of dielectric is observed and the breakdown occurs at 1.2 MV/cm. The in-situ XPS analysis of C_{1s} spectra reveals O_2 plasma pretreatment could break sp_2 hybridization and make the surface hydrophilic for the following ALD process. These results will provide a new solution for future application in graphene based devices that could be compatible with the CMOS fabrication process.

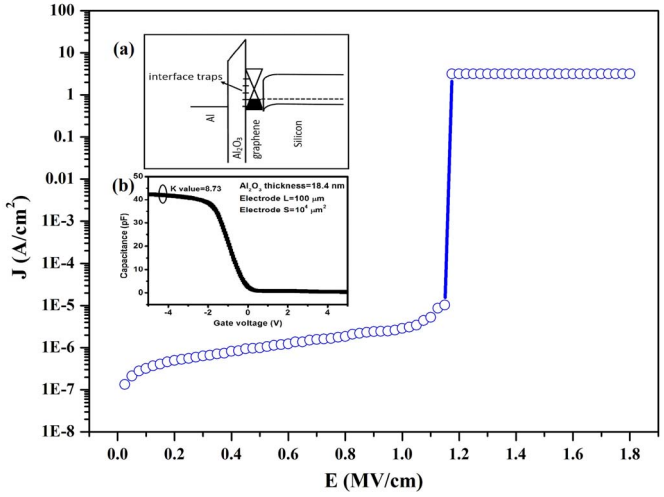

Figure 4 | **The current density versus the electric field (J-E) characteristics of Al/Al_2O_3/graphene/Si structure.** Insert: (a) a schematic band-diagram of the structure when Al is biased to a positive voltage, (b) the C-V curve of the structure.

Methods

The graphene was synthesized by the Cu-catalyzed low-pressure chemical vapor deposition. Following this synthesis, graphene was transferred by spin-coating a "handle" layer which comprises of poly (methylmethacrylate (PMMA)). The PMMA layer was used to support the graphene film while the Cu substrate was etched in $FeCl_3$. The obtained PMMA/graphene membrane was then transferred to a highly-doped silicon substrate. After removing PMMA with acetone, cleaning and drying, the graphene/n+-Si sample was transferred to ALD chamber. The whole ALD process with remote O_2 plasma surface pretreatment was undertaken in the Picosun R200 system. After remote O_2 plasma exposure for 20 seconds (s), Al_2O_3 was deposited at ~250°C using TMA and water as precursors for 200 cycles. The pulse time for TMA was 0.1 s, which is followed by a 6 s purge, 0.1 s H_2O pulse and 10 s purge. The resulting growth rate was about 0.1 nm/cycle and the obtained Al_2O_3 film thickness was about 20 nm. In order to evaluate the quality of the dielectric in electrical characteristics, we made top electrodes using sputtering and the electrode thickness was about 100 nm. The top electrodes made of Al were formed by hard mask with a radius of 100 μm.

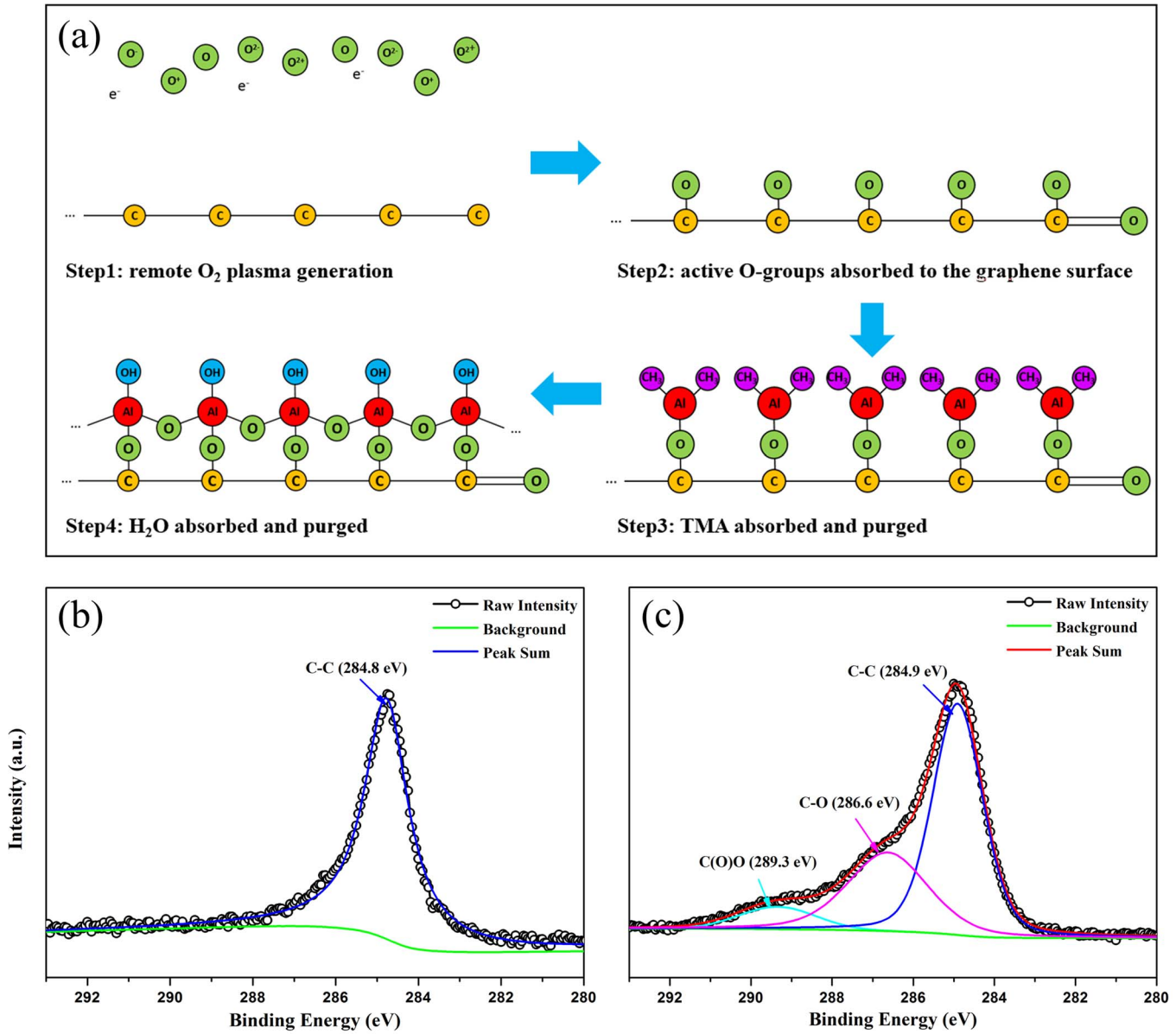

Figure 5 | (a) The dynamic mechanism of Al_2O_3 dielectric forming on top of graphene by remote O_2 plasma pretreated ALD. The in-situ XPS of C_{1s} spectra of (b) before and (c) after oxygen plasma treatment.

1. Frank, S. Graphene transistors. *Nat. Nanotechnol.* **5**, 487–496 (2010).
2. Novoselov, K. S. *et al.* A roadmap for graphene. *Nature* **490**, 192–200 (2012).
3. Geim, A. K. Graphene: Status and Prospects. *Science* **324**, 1530–1534 (2009).
4. Lin, Y. *et al.* Operation of Graphene Transistors at Gigahertz Frequencies. *Nano Lett.* **9**, 422–426 (2009).
5. Kim, K., Choi, J. Y., Kim, T., Cho, S. H. & Chung, H. J. A role for graphene in silicon-based semiconductor devices. *Nature* **479**, 338–344 (2011).
6. Hong, S. K., Kim, J. E., Kim, S. O., Choi, S. Y. & Cho, B. J. Flexible resistive switching memory device based on graphene oxide. *IEEE Electron. Dev. Lett.* **31**, 1005–1007 (2010).
7. Jeong, H. Y. *et al.* Graphene oxide thin films for flexible nonvolatile memory applications. *Nano Lett.* **10**, 4381–4386 (2010).
8. Sprinkle, M. *et al.* Scalable templated growth of graphene nanoribbons on SiC. *Nat. Nanotechnol.* **5**, 727–731 (2010).
9. Fallahazad, B. *et al.* Scaling of Al2O3 dielectric for graphene field-effect transistors. *Appl. Phys. Lett.* **100**, 093112 (2012).
10. Wang, X. R., Tabakman, S. M. & Dai, H. J. Atomic Layer Deposition of Metal Oxides on Pristine and Functionalized Graphene. *J. Amer. Chem. Soc.* **130**, 8152–8153 (2008).
11. Justice, M. P. *et al.* Seeding Atomic Layer Deposition of High-k Dielectrics on Epitaxial Graphene with Organic Self-Assembled Monolayers. *ACS Nano* **5**, 5223–5232 (2011).
12. Liu, N. *et al.* The Origin of Wrinkles on Transferred Graphene. *Nano Res.* **4**, 996–1004 (2011).
13. Ferrari, A. C. *et al.* Raman spectrum of graphene and graphene layers. *Phys. Rev. Lett.* **97**, 187401 (2006).
14. Gupta, A., Chen, G., Joshi, P., Tadigadapa, S. & P. C. Raman scattering from high-frequency phonons in supported n-graphene layer films. *Nano Lett.* **6**, 2667–2673 (2006).
15. Dresselhaus, M. S. *et al.* Perspectives on Carbon Nanotubes and Graphene Raman Spectroscopy. *Nano Lett.* **10**, 751–758 (2010).
16. Andrea, C. F. Raman spectroscopy of graphene and graphite: Disorder, electron-phonon coupling, doping and nonadiabatic effects. *Solid State Commun.* **143**, 47–57 (2007).
17. Yan, Z. *et al.* Growth of bilayer graphene on insulating substrates. *ACS Nano* **5**, 8187–8192 (2011).
18. Peng, Z. W., Yan, Z., Sun, Z. Z. & James, M. T. Direct growth of bilayer graphene on sio2 substrates by carbon diffusion through nickel. *ACS Nano* **5**, 8241–8247 (2011).
19. Shahin, A. M. *et al.* A comprehensive study on the leakage current mechanisms of Pt/SrTiO3/Pt capacitor. *J. Appl. Phys.* **111**, 014503 (2012).
20. Sherrill, S. A., Banerjee, P., Rubloff, G. W. & Lee, S. B. High to ultra-high power electrical energy storage. *Phys. Chem. Chem. Phys.* **13**, 20714–23 (2011).

21. Tang, L. H. *et al*. Preparation, Structure, and Electrochemical Properties of Reduced Graphene Sheet Films. *Adv. Funct. Mater.* **19**, 2782–2789 (2009).
22. Yang, D. X. *et al*. Chemical analysis of graphene oxide films after heat and chemical treatments by X-ray photoelectron and Micro-Raman spectroscopy. *Carbon* **47**, 145–152 (2009).

Acknowledgments

This work was supported by the National Natural Science Foundation of China (61376093), Shanghai Municipal Science and Technology Commission (13QA1400400), National Science and Technology Major Project (2011ZX02707) and Innovation Program of Shanghai Municipal Education Commission (12ZZ010).

Author contributions

P.Z. and S.B.Y. contribute to performing the experiment and drafting the manuscript. Q.Q.S. and L.C. contribute to designing this research and analyzing the results. S.J.D., P.F.Wang and D.W.Z. analyzed the data and discussed the results. All authors reviewed the manuscript.

Additional information

Competing financial interests: The authors declare no competing financial interests.

How to cite this article: Zhou, P. *et al*. Direct Deposition of Uniform High-κ Dielectrics on Graphene. *Sci. Rep.* **4**, 6448; DOI:10.1038/srep06448 (2014).